

Radiation doses to brain substructures associated with cognition in radiotherapy of pediatric brain tumors

Laura Toussaint^a, Daniel J. Indelicato^b , Camilla H. Stokkevåg^c, Yasmin Lassen-Ramshad^a, Catia Pedro^d, Ronni Mikkelsen^e, Marcos Di Pinto^b, Zuofeng Li^b, Stella Flampouri^b, Anne Vestergaard^a, Jørgen B. B. Petersen^a, Henrik Schrøder^f, Morten Høyer^a and Ludvig P. Muren^a

^aDanish Centre for Particle Therapy, Aarhus, Denmark; ^bDepartment of Radiation Oncology, University of Florida, Jacksonville, FL, USA; ^cDepartment of Oncology and Medical Physics, Haukeland University Hospital, Bergen, Norway; ^dDepartment of Radiotherapy, Instituto Português de Oncologia de Lisboa Francisco Gentil, EPE, Lisbon, Portugal; ^eDepartment of Neuroradiology/Biomedicine, Aarhus University Hospital, Aarhus, Denmark; ^fDepartment of pediatrics, Aarhus University Hospital, Aarhus, Denmark

ABSTRACT

Background: Several brain substructures associated with cognition (BSCs) are located close to typical pediatric brain tumors. Pediatric patients therefore have considerable risks of neurocognitive impairment after brain radiotherapy. In this study, we investigated the radiation doses received by BSCs for three common locations of pediatric brain tumor entities.

Material and methods: For ten patients in each group [posterior fossa ependymoma (PFE), cranio-pharyngioma (CP), and hemispheric ependymoma (HE)], the cumulative fraction of BSCs volumes receiving various dose levels were analyzed. We subsequently explored the differences in dose pattern between the three groups and used available dose response models from the literature to estimate treatment-induced intelligence quotient (IQ) decline.

Results: Doses to BSCs were found to differ considerably between the groups, depending on their position relative to the tumor. Large inter-patient variations were observed in the ipsilateral structures of the HE groups, and at low doses for all three groups. IQ decline estimates differed depending on the model applied, presenting larger variations in the HE group.

Conclusion: While there were notable differences in the dose patterns between the groups, the extent of estimated IQ decline depended more on the model applied. This inter-model variability should be considered in dose–effect assessments on cognitive outcomes of pediatric patients.

ARTICLE HISTORY

Received 10 April 2019
Accepted 25 May 2019

Introduction

Central nervous system (CNS) tumors are the second most common cancer in children [1]. During the last decade, survival rates have improved, primarily due to the multimodality treatment of the disease [2]. However, pediatric cancer survivors are at increased risk of developing long-term morbidity after therapy, compromising their quality of life. Recent data from the St. Jude Lifetime Cohort Study reported that among children with cancer, survivors of CNS malignancies have the highest cumulative burden of chronic health conditions of any grade, and significantly higher burdens than the general population [1].

Childhood CNS cancer survivors often suffer from cognitive impairment including deficits in working memory, attention, and/or processing speed [3–5]. Radiotherapy (RT) associated neurocognitive impairment can arise from different mechanisms, including white matter and brain plasticity changes, vascular damage or decreased neurogenesis [6,7]. Structural brain changes (i.e. grey/white matter changes) have been associated to a broad range of neurocognitive

outcomes [8]. However, while some cerebral cortex regions have been shown to be more sensitive to radiation in adult brain tumor patients [9], evidence is still needed in pediatric patients. Moreover, the pediatric population differs from adults, e.g. with greater degrees of neurogenesis and myelination of white matter tracts.

Most studies investigating associations between radiation doses and cognition in children have focused on craniospinal irradiation of posterior fossa tumors [10,11]. Merchant et al. quantified the association between intelligence quotient (IQ) scores and doses to large brain regions such as the temporal lobes, supratentorial brain, or the whole brain for four typical pediatric brain tumors [12]. Armstrong et al. focused on the same large structures, and their association to functional impairments [13]. Redmond et al. prospectively investigated the association between radiation dose, cognitive function, and corpus callosum substructures [14] or neural progenitor cell niches [15]. In recent studies, it has been shown that dose/volume parameters of smaller brain structures have a stronger association with cognitive decline than larger brain

regions, e.g. the left hippocampus rather than the left temporal lobe with respect to memory scores [16].

The overall aim of this study was therefore to investigate the pattern of radiation doses delivered to a broad range of potential cognitive brain structures in pediatric patients with three common CNS tumor entities arising in typical brain locations. Applying the available dose-response models based on dose/volume parameters from large brain regions, we further investigated the differences across patient groups with respect to predicted IQ decline following RT.

Material and methods

Patient material and treatment planning

Thirty anonymized pediatric patients previously treated for CNS tumors at the University of Florida Health (Jacksonville, FL, USA) were included in this institutional review board approved study: ten with posterior fossa ependymoma (PFE), ten with craniopharyngioma (CP), and ten with hemispheric ependymoma (HE). The PFE tumors were located in the cerebellum/4th ventricle, with a median primary planning target volume (PTV1) of 42 cm³ (26–62 cm³). CP tumors were suprasellar, central to brain substructures associated with cognition (BSCs), with a median PTV1 of 31 cm³ (18–66 cm³). For the HE patients, the tumors were lateralized in the supratentorial cerebrum (four left and six right cases), with a median PTV1 of 97 cm³ (31–147 cm³) for the right hemisphere tumors and 77 cm³ (45–192 cm³) for the left hemisphere. All patients were replanned with Volumetric Modulated Arc Therapy (VMAT), based on the clinically approved structure sets; i.e. the additional BSCs delineated for this study (see next section) were not included in the optimization. More information on the planning process are available in [Supplementary Material](#).

Brain substructures associated with cognition

A total of thirty BSCs were investigated, based on their potential association to cognitive function [7]. Delineation of

the supratentorial brain, temporal lobes and hippocampal head and tail were available in the clinical structure sets, based on the Children's Oncology Group guidelines. The remaining BSCs were delineated by experienced radiation oncologists and a neuroradiologist from co-registered T1 magnetic resonance imaging (MRI) and planning computed tomography (CT) scans. The BSCs along with the references used for delineation are shown in [Table 1](#).

The brain was first divided into the supratentorial brain, a region where radiation doses have been associated to IQ decrease in pediatric radiation therapy patients [12], and the cerebellum. The supratentorial part was further delineated as right and left hemispheres, including the frontal, parietal and temporal lobes. Based on results from Merchant et al., the cerebellum was separated into its anterior and posterior sections for its association to IQ scores [23], but also to functional loops as for example the cerebello-thalamo-cortical loop and its role in working memory [24]. We also delineated the corpus callosum that acts as a connecting bridge between hemispheres and is therefore important for processing speed [14]. For regions with a strong role in neurogenesis, we investigated the subventricular zones as well as the hippocampus [15]. The hippocampus has also been related to working and spatial memory functions. Other BSCs assumed to be important for memory included the amygdala (emotional memory [19]), the thalamus, as well as the entorhinal cortices [20] and the Circuit of Papez [22] (see [Supplementary Material](#)). Finally, the left frontal white matter horn was delineated for its role in executive function [7].

Data analysis

Dose volume histograms of the BSCs were calculated using the Eclipse planning system (version 13.7, Varian Medical Systems, Palo Alto, CA, USA). We derived the cumulative fraction of volume receiving low (V10Gy, V20Gy), intermediate (V30Gy, V40Gy) and high (V50Gy, V60Gy) doses. Comparison between the three groups was addressed by calculating the difference in median values, for all dose levels and BSCs.

Table 1. Brain substructures associated with cognition included in the study with respective delineation guidelines.

	Structure	Contouring guidelines
	Brain	Clinical structure set [17]
	Brain supratentorial	Clinical structure set [17]
Posterior fossa substructures	Cerebellum (anterior/posterior)	[17,18]
Temporal lobe substructures	Hippocampus (head/tail)	Clinical structure set [19]
	Amygdala	[19]
	Entorhinal cortex	[20], Supplementary material
Ventricular substructures	Subventricular zone	[7,21]
	Cingulum	Supplementary material
	Fornix	Supplementary material
	Corpus callosum	[7]
Other supratentorial substructures	Frontal lobe	Atlas of Human Anatomy, Netter
	Parietal lobe	Atlas of Human Anatomy, Netter
	Temporal lobe	Clinical structure set [17]
	Left frontal white matter	[7]
	Thalamus	Atlas of Human Anatomy, Netter
Circuit of Papez	Neural circuit: hippocampus, entorhinal cortex, fornix, cingulum, anterior nucleus of the thalamus, mammillary bodies and mammillothalamic tract	[22] Supplementary material

To estimate the effects of the delivered doses on cognitive function, we applied three published dose response models of IQ score after RT, available in the literature, to our patient population. The three models were developed by Merchant et al. [25,26], and details on the models are presented in [Supplementary Material](#).

Wilcoxon ranked-sum test (significance level $p < 0.05$) were performed to compare the IQ score estimates and dose/volume parameters across groups. For the dose/volume parameters assessment, the significance level was set to $p < 0.008$ after Bonferroni correction for multiple testing within each BSCs (i.e. correction for testing the six different dose levels).

Results

Dose patterns depending on tumor location

In the PFE group, the cerebellum substructures were the only BSCs exposed to intermediate and high dose levels. The temporal lobe and its substructures were exposed to low doses, with a V10Gy of 100% for the entorhinal cortices and left hippocampus head. In addition, large variations were seen between patients at low dose levels, e.g. with very large range variations for the V10Gy parameter of all temporal lobe substructures. The BSCs located in the superior part of the supratentorial brain were spared from receiving 10 Gy or more in all patients, as confirmed by the low range values ([Figure 1](#)).

The CP group presented the most heterogeneous dose patterns, due to the central location of the target as a function of BSCs. The temporal lobe BSCs received large fractions of low doses, with notably V10Gy being 100% for all of them with no variation in range (close to 0%), illustrating a common trend across all patients. The ventricular BSCs were in general spared from intermediate to high doses, as opposed to the amygdala and entorhinal cortex, in the closest vicinity of the PTV. However, large variations were seen between patients: for the ventricular BSCs, the largest variations were seen at low doses, while for the temporal lobe BSCs the variations were mostly observed for intermediate (e.g. hippocampus and substructures) to high doses (e.g. amygdala, entorhinal cortices) ([Figure 1](#)).

In the HE group, the substructures of the temporal lobes and posterior fossa received very little dose with all median V10Gy values below 5%. The ventricular substructures as well as the bilateral parietal and frontal lobes were mostly exposed to the low dose levels, with a median V10Gy of 48% for the corpus callosum. However, the volume range was up to 100% for most of the temporal lobe and ventricular substructures, reflecting large heterogeneities across the group ([Figure 1](#)).

When separating the patients with HE by tumor lateralization, different patterns could be seen ([Supplementary Figure S1](#)). The ipsilateral BSCs presented the largest variations between patients across all dose levels for the left HE group, and mostly at low dose levels in the right HE group. For both lateralization, the contralateral temporal lobe and its substructures were in general spared from radiation, as well as the cerebellum substructures. Small variations were seen

between patients, with range values close to 0% in both groups and across all dose levels. The parietal and frontal lobes as well as the ventricular substructures were exposed to the highest levels of low to intermediate doses, reaching 90% for the right parietal lobe (right HE group) and around 80% for the corpus callosum, left cingulum, left subventricular zone, and the circuit of Papez (left HE group). There were large dose variations across the HE group in the ventricular BSCs, with ranges reaching 90% across all dose levels for the left HE group.

A summary of the differences between the three groups can be seen in [Supplementary Figure S2](#).

Estimated IQ decline

The IQ change at 24 months after RT was statistically significantly different between the three groups only when estimated from the general ependymoma model. In the PFE and CP groups, both the general and posterior fossa ependymoma models showed a trend towards a larger decline in IQ for the patients with the smallest PTV volumes. When comparing across the three groups, no differences were seen in estimates from the PFE model ($p > 0.05$). Overall, the craniopharyngioma model estimated the largest decline (around ten IQ points) for all patients but one (the left HE patient with the largest PTV, who notably had an increase in IQ score after RT) ([Figure 2](#)).

In the PFE group, the estimates from the three models followed the same overall trend, with the posterior fossa ependymoma model indicating the smallest changes in IQ score and the craniopharyngioma model the largest. In the CP group, the general ependymoma model estimated the smallest decline, and in particular improvement in IQ score for the two patients with the largest PTV volumes, whereas the patient with the largest PTV volume had the largest decline in IQ (ten points) when calculated from the posterior fossa ependymoma model. In the HE group, more variations were observed between the models. The craniopharyngioma model estimated consistently reduced IQ score 24 months after RT, whereas the general ependymoma model estimated an improved IQ score, in particular for the largest tumors in both the left and right HE groups. The posterior fossa ependymoma model scores were highly variable across the ten patients, and seemingly independent of the PTV volumes ([Figure 2](#)).

Discussion

The major contribution of this study was the systematic and comprehensive approach in delineating a broad range of brain substructures potentially associated with radiation-induced cognitive decline. Indeed, there is growing interest concerning the influence of more specific brain substructures on cognitive function and the observed outcomes after RT [5,10,14,16]. Overall we found that the doses to the temporal lobe substructures had the largest variations both between and within all explored groups, with statistically significant differences between the CP group and the two ependymoma

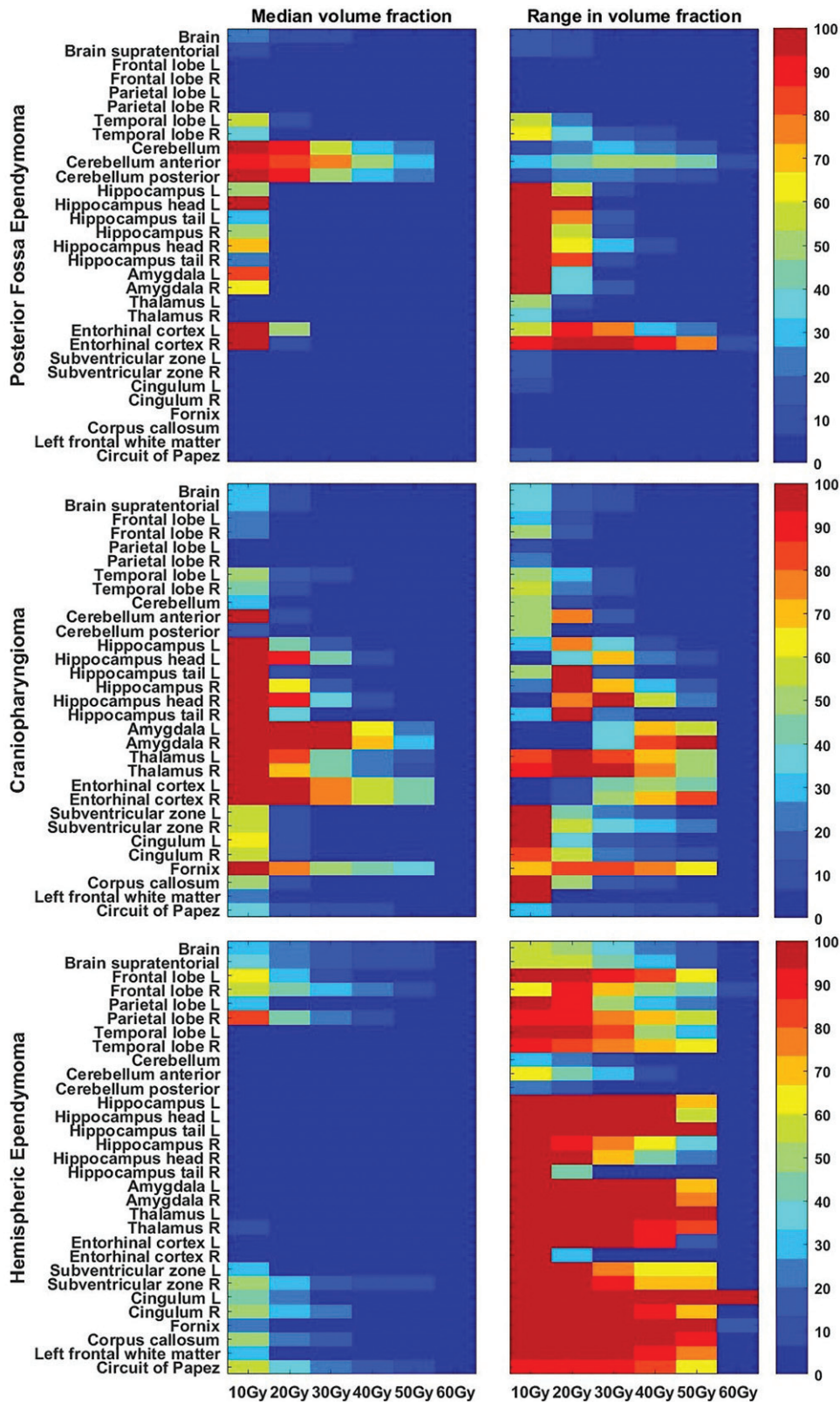


Figure 1. Median volume (left column, %) and volume range (right column, %) of the fraction of BSCs volume exposed to different dose levels, the warmest colors representing the highest volume exposure/variations across the group.

groups. Notably, details of the dose distribution are also important at low dose levels, as it has been reported that low doses delivered to the brain of pediatric patients could have detrimental effects on cognition in adulthood [27]. Segmenting the substructures of each temporal lobe might

therefore capture more detailed information than considering the temporal lobe as one structure.

Most of the published models of neurocognitive impairment after RT are derived using broad dose intervals from large brain regions. Different internal dose distributions was

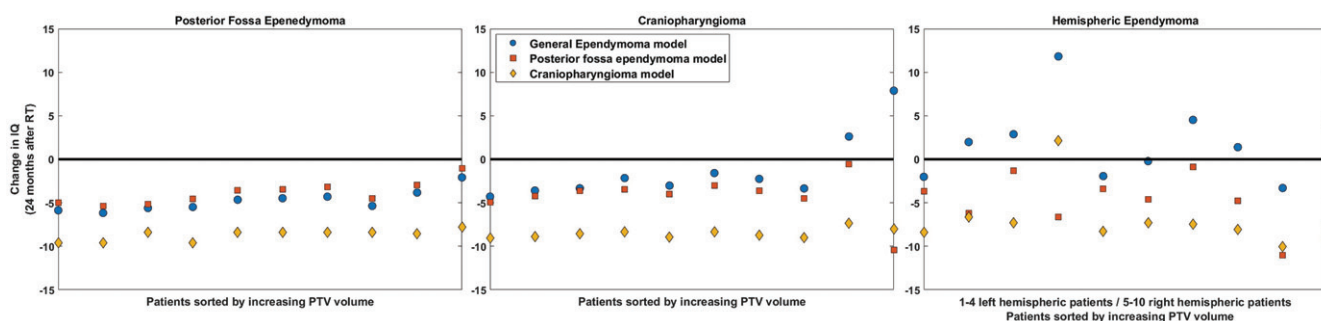


Figure 2. Estimated IQ change 24 months after RT for each patient group, based on three different combinations of supratentorial brain dose/volume endpoints available in the literature.

found to result in similar IQ estimates when calculated from large supratentorial brain dose/volume-intervals. For example, the craniopharyngioma model [26] predicted similar IQ scores the three groups whereas the dose patterns varied considerably for all dose levels and cognitive substructures, as well as between patients. Again this suggests that smaller BSCs are capturing more nuanced information on dose variation than large brain regions, and might therefore be used to develop more sensitive outcome models for radiation-induced cognitive impairment. With this aim, systematic neurocognitive testing of pediatric CNS tumor patients would be a first step towards better dose/volume model development.

Improved understanding of the pattern of doses delivered to BSCs could be helpful when designing clinical studies, e.g. to define which specific cognitive function to monitor depending on the tumor location and its associated dose patterns, as proposed by McDonald et al. [28]. For example, patients with HE could be used to study the left hemisphere prevalence on cognitive outcomes [16,28], with a comparison of right vs. left sided tumor groups, all presenting contralateral hemisphere sparing.

Despite being a descriptive study based on a small sample size, the dose patterns we report appear generalizable across PFE and CP groups, providing insight into which BSCs are the most exposed to specific dose levels during intensity modulated RT. Moreover, we could expand the observed dose patterns to tumors with the same anatomical location; e.g. low grade glioma of the optic pathway compared to CP, or the boost volume of medulloblastoma and PFE. In the PFE and CP groups, most of the variation between patients may be attributed to differences in target volume, whereas in the HE group there were additional differences in tumor laterality and tumor depth within the supratentorial brain.

In this study, we applied population-specific models to different patient groups. The generalizability of the models across different tumor types is questionable, given the differences between the cohorts that may influence the outcome. For example, the youngest patients at time of RT have higher risks of cognitive impairment. Therefore, the differences in incidence age between the groups (i.e. median age at diagnosis PFE/HE 3 years old vs. CP 7 years old; [Supplementary Table S1](#)) would have a large impact on the changes in IQ score. By calculating the change in IQ relative to baseline,

these estimates were made independent of age and could therefore focus on the direct impact of the dose parameters on the estimated outcome.

The three models used in this study were fitted from 3D conformal RT data. Large differences exist between 3D conformal RT and VMAT in term of dose distribution: there is a general increase in low dose volumes and a reduction in the intermediate and high dose volumes with VMAT. Paradoxically, in our cohort, patients with the largest tumor volumes presented more favorable IQ scores despite that larger brain volumes received high doses. These results may imply that the use of such models should be limited to the specific delivery technique that the models were based on, with its characteristic dose distribution.

It should be noted that the Merchant et al. studies referred to an estimated IQ (EIQ) score, which did not include processing speed estimates as opposed to FSIQ. This difference in endpoints has been discussed recently by Burgess et al. [29]. They emphasized that EIQ scores could be underestimating the effects of RT on the brain compared to using FSIQ scores, as the processing speed (one of the main function impaired over time in pediatric brain tumor survivors), was disregarded [5,29]. Comparisons of estimates from different models should therefore be done with caution.

Moreover, IQ score is not necessarily an adequate endpoint when investigating neurocognitive changes after RT, as it does not carry information on the structure-function relations of the brain. In addition, the temporal variation in IQ changes may be complicated by transient effects at the time of treatment (e.g. hydrocephalus and other complications) which may resolve after completion of treatment, leading to a short-term rebound or improvement in scores. Monitoring specific functions (such as processing speed or working memory) could give more insight into the effects of radiotherapy on brain structure–function relation, as demonstrated for example for the hippocampus and memory [16].

In summary, our study demonstrated that the pattern of doses to the BSCs differed considerably between the three groups, depending on the tumor location. However, these dose variations were not reflected in the IQ estimates. Overall, delineation of more brain structures and systematic cognitive testing of pediatric CNS patients could refine dose-constraints and drive estimation of new predictors of cognitive impairment.

Disclosure statement

The authors have no conflicts of interest to disclose.

Funding

The authors acknowledge the Danish Cancer Research Fund, the Danish Cancer Society and Aarhus University for financial support of this work.

ORCID

Daniel J. Indelicato  <http://orcid.org/0000-0001-5765-1873>

References

- [1] Bhakta N, Liu Q, Ness KK, et al. The cumulative burden of surviving childhood cancer: an initial report from the St Jude Lifetime Cohort Study (SJLIFE). *Lancet*. 2017;390:2569–2582.
- [2] Breneman JC, Donaldson SS, Constine L, et al. The children's oncology group radiation oncology discipline: 15 years of contributions to the treatment of childhood cancer. *Int J Radiat Oncol Biol Phys*. 2018;101:860–874.
- [3] Brinkman TM, Krasin MJ, Liu W, et al. Long-term neurocognitive functioning and social attainment in adult survivors of pediatric CNS tumors: results from the St Jude lifetime cohort study. *J Clin Oncol*. 2016;34:1358–1367.
- [4] Ellenberg L, Liu Q, Gioia G, et al. Neurocognitive Status in long-term survivors of childhood CNS malignancies: a Report From the Childhood Cancer Survivor Study. *Neuropsychology*. 2009;23:705–717.
- [5] Padovani L, André N, Constine LS, et al. Neurocognitive function after radiotherapy for paediatric brain tumours. *Nat Rev Neurol*. 2012;8:578–588.
- [6] Makale MT, McDonald CR, Hattangadi-Gluth JA, et al. Mechanisms of radiotherapy-associated cognitive disability in patients with brain tumours. *Nat Rev Neurol*. 2017;13:52–64.
- [7] Peiffer AM, Leyrer CM, Greene-Schloesser DM, et al. Neuroanatomical target theory as a predictive model for radiation-induced cognitive decline. *Neurology*. 2013;80:747–753.
- [8] Ailion AS, Hortman K, King TZ. Childhood brain tumors: a systematic review of the structural neuroimaging literature. *Neuropsychol Rev*. 2017;27:220–244.
- [9] Seibert TM, Karunamuni R, Kaifi S, et al. Cerebral cortex regions selectively vulnerable to radiation dose-dependent atrophy. *Int J Radiat Oncol Biol Phys*. 2017;97:910–918.
- [10] Doger de Speville E, Robert C, Perez-Guevara M, et al. Relationships between regional radiation doses and cognitive decline in children treated with crani-spinal irradiation for posterior fossa tumors. *Front Oncol*. 2017;7:166.
- [11] Blomstrand M, Brodin NP, Munck AF, Rosenschöld P, et al. Estimated clinical benefit of protecting neurogenesis in the developing brain during radiation therapy of pediatric medulloblastoma. *Neuro Oncol*. 2012;14:882–889.
- [12] Merchant TE, Kiehna EN, Li C, et al. Modeling radiation dosimetry to predict cognitive outcomes in pediatric patients with CNS embryonal tumors including medulloblastoma. *Int J Radiat Oncol Biol Phys*. 2006;65:210–221.
- [13] Armstrong GT, Jain N, Liu W, et al. Region-specific radiotherapy and neuropsychological outcomes in adult survivors of childhood CNS malignancies. *Neuro Oncol*. 2010;12:1173–1186.
- [14] Redmond KJ, Hildreth M, Sair HI, et al. Association of neuronal injury in the genu and body of corpus callosum after cranial irradiation in children with impaired cognitive control: a prospective study. *Int J Radiat Oncol Biol Phys*. 2018;101:1234–1242.
- [15] Redmond KJ, Mahone EM, Terezakis S, et al. Association between radiation dose to neuronal progenitor cell niches and temporal lobes and performance on neuropsychological testing in children: a prospective study. *Neuro Oncol*. 2013;15:360–369.
- [16] Zureick AH, Evans CL, Niemierko A, et al. Left hippocampal dosimetry correlates with visual and verbal memory outcomes in survivors of pediatric brain tumors. *Cancer*. 2018;124:2238–2245.
- [17] Eekers DB, In't Ven L, Roelofs E, et al. The EPTN consensus-based atlas for CT- and MR-based contouring in neuro-oncology. *Radiation Oncol*. 2018;128:37–43.
- [18] Eekers DBP, In't Ven L, Deprez S, et al. The posterior cerebellum, a new organ at risk? *Clin Transl Radiat Oncol*. 2018;8:22–26.
- [19] Chera BS, Amdur RJ, Patel P, et al. A radiation oncologist's guide to contouring the hippocampus. *Am J Clin Oncol*. 2009;32:20–22.
- [20] Insausti R, Juottonen K, Soininen H, et al. MR volumetric analysis of the human entorhinal, perirhinal and temporopolar cortices. *AJNR AM J Neuroradiol*. 1998;19:659–671.
- [21] Barani IJ, Cuttino LW, Benedict SH, et al. Neural stem cell-preserving external-beam radiotherapy of central nervous system malignancies. *Int J Radiat Oncol Biol Phys*. 2007;68:978–985.
- [22] Papez JW. A proposed mechanism of emotion. *Arch Neuropsychol*. 1937;38:725–743.
- [23] Merchant TE, Sharma S, Xiong X, et al. Effect of cerebellum radiation dosimetry on cognitive outcomes in children with infratentorial ependymoma. *Int J Radiat Oncol Biol Phys*. 2014;90:547–553.
- [24] Law N, Bouffet E, Laughlin S, et al. Cerebello-thalamo-cerebral connections in pediatric brain tumor patients: impact on working memory. *Neuroimage*. 2011;56:2238–2248.
- [25] Merchant TE, Kiehna EN, Li C, et al. Radiation dosimetry predicts IQ after conformal radiation therapy in pediatric patients with localized ependymoma. *Int J Radiat Oncol Biol Phys*. 2005;63:1546–1554.
- [26] Merchant TE, Kiehna EN, Kun LE, et al. Phase II trial of conformal radiation therapy for pediatric patients with craniopharyngioma and correlation of surgical factors and radiation dosimetry with change in cognitive function. *J Neurosurg Pediatr*. 2006;104:94–102.
- [27] Hall P, Adami H-O, Trichopoulos D, et al. Effect of low doses of ionising radiation in infancy on cognitive function in adulthood: Swedish population based cohort study. *Br Med J*. 2004;328:19–0.
- [28] McDonald AM, Murdaugh DL, Milner D, et al. Brain dosimetry from locally advanced head and neck cancer radiotherapy: implications for neurocognitive outcomes research. *Acta Oncol*. 2018;57:1589–1592.
- [29] Burgess L, Pulsifer MB, Grieco JA, et al. Estimated IQ systematically underestimates neurocognitive sequelae in irradiated pediatric brain tumor survivors. *Int J Radiat Oncol Biol Phys*. 2018;101:541–549.